6.8 Cavity Design and Analysis

The cavity consists of components directly surrounding the exploding targets, including the first wall, blanket, coolant manifolding, vacuum vessel, and shield. These components contain the energy of the blast, absorb the neutrons produced, convert energy into usable heat, breed tritium to sustain the DT fuel cycle, and shield components and personnel from the high radiation environment. Thus, it has a central role in determining the major attributes of the reactor, such as cost, safety and environmental features, engineering attractiveness, and technical feasibility.

Several fundamental principles were established at the beginning of the cavity design process and guided the major study design decisions. The final design results from a large number of trade-offs which incorporated these design goals.

A top priority was the desire for inherent safety and minimum activation. This desire influenced material choices for the first wall, blanket, and shield. The first wall employes low-activation SiC composite. Both long-term and short-term activation is small, thus minimizing waste disposal problems and providing negligible decay heat. Li and LiPb were rejected for safety reasons in favor of a Pb wall protectant. Pb has toxicity and radioactivity concerns, but these were carefully estimated and minimized in the design. The blanket also uses SiC structure and reflector, with low-activation Li_2O breeder and He coolant. The tritium inventory in the breeder was minimized . Use of He at relatively low pressure, together with multiple containment barriers, maked blanket failures unlikely and the consequences benign. The shield material also was chosen to reduce activation. Instead of concrete, Prometheus uses an innovative, highly-effective shield consisting of Al structure, water coolant, and B_4C, Pb, and SiC absorbers.

Another major guiding principle was the incorporation of a sound engineering basis. While not all of the design choices use proven technologies, an attempt was made to minimize required R&D and technical risk by adopting near-term technologies that can be extrapolated from existing data. SiC composites are commercially available today, although some development will be required for use in a neutron radiation environment. Pb has been used as a coolant in the past and technologies for using liquid metal as a coolant are well-developed. Similarly, in the blanket, He cooling is an established technology. The data base for Li_2O is being rapidly developed for the MFE fusion program. While not a driving force in the design, the relevance of Prometheus technology to MFE allows an effective R&D program to be developed with minimum cost and time to completion. The R&D needs are bounded and predictable, since the extrapolation from existing technologies is minimized. Cost penalties can be expected as compared with design concepts which are novel, or even radical; however, this was judged to be a reasonable strategy given the time schedule for fusion development.

The Prometheus design concept and configuration were chosen following a careful review of existing designs in both the IFE and MFE literature. The design options considered are described in more detail in Chapter 4. Following this survey, a wetted-wall design was adopted with separate first wall and blanket. Wetted walls have many potential engineering advantages, including good beamline accommodation, relaxed repetition rate limitations (as compared with thick films), flexible engineering features, and low inventory and flow rate of the liquid film.

Figures 6.8-1 and 6.8-2 show perspective views of the cavity with and without laser beams. The overall configuration of Prometheus is a low aspect ratio cylinder with hemispherical end caps. This configuration was selected for several reasons:

(1) Maintenance of a cylinder is easier than a sphere. Maintenance paths are all straight vertical lines and the configuration allows independent removal of FW panels and blanket modules.
(2) A cylinder provides better control of film flow. Problems protecting the upper hemisphere can be reduced with higher aspect ratio, in which the distance from the blast to the upper end cap can be maximized.
(3) A cylindrical configuration is more consistent with conventional plant layouts.

The main disadvantage of this concept is nonuniform power distribution and higher peak loads. The higher peak-to-average loading leads to larger size and higher cost for a given total reactor power. To minimize these disadvantages, the aspect ratio is kept relatively low—of the order of 1-2; however, this also limits the advantage of upper end cap protection.

The wall protection scheme chosen for Prometheus uses a thin liquid Pb film supplied from Pb coolant tubes through a porous structure of SiC composite material. The first wall coolant must have acceptable neutronic properties (either breed, multiply neutrons, or be transparent), such that the choices are limited to Li-bearing materials and neutron multipliers. Pb was selected for a number of reasons. Pb has a safety advantage over Li, good neutron multiplication, and chemical compatability with SiC. Its thermophysical properties provide good operating temperature ranges. Its relatively high saturation temperature leads to good conduction heat transfer into the coolant, its boiling point is not too high for materials temperature limits and compatibility, and the relatively high bulk coolant temperature gives good thermal conversion efficiency. Bi and BiPb were considered as alternate multipliers, but they have much higher radioactivity. Some of the outstanding disadvantages of Pb include high density and activation.

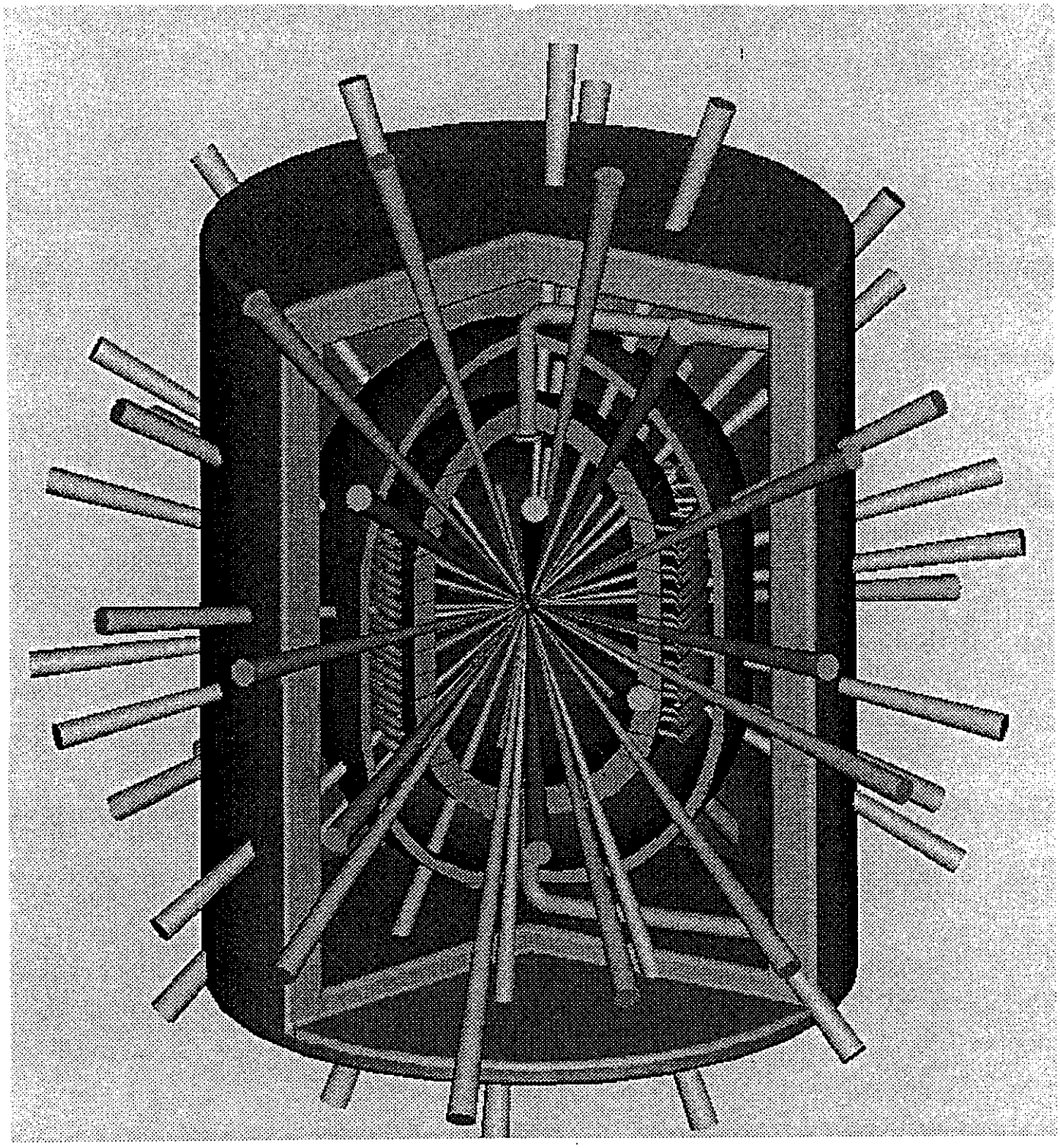

Figure 6.8-1. Perspective View of the Cavity with Laser Beams

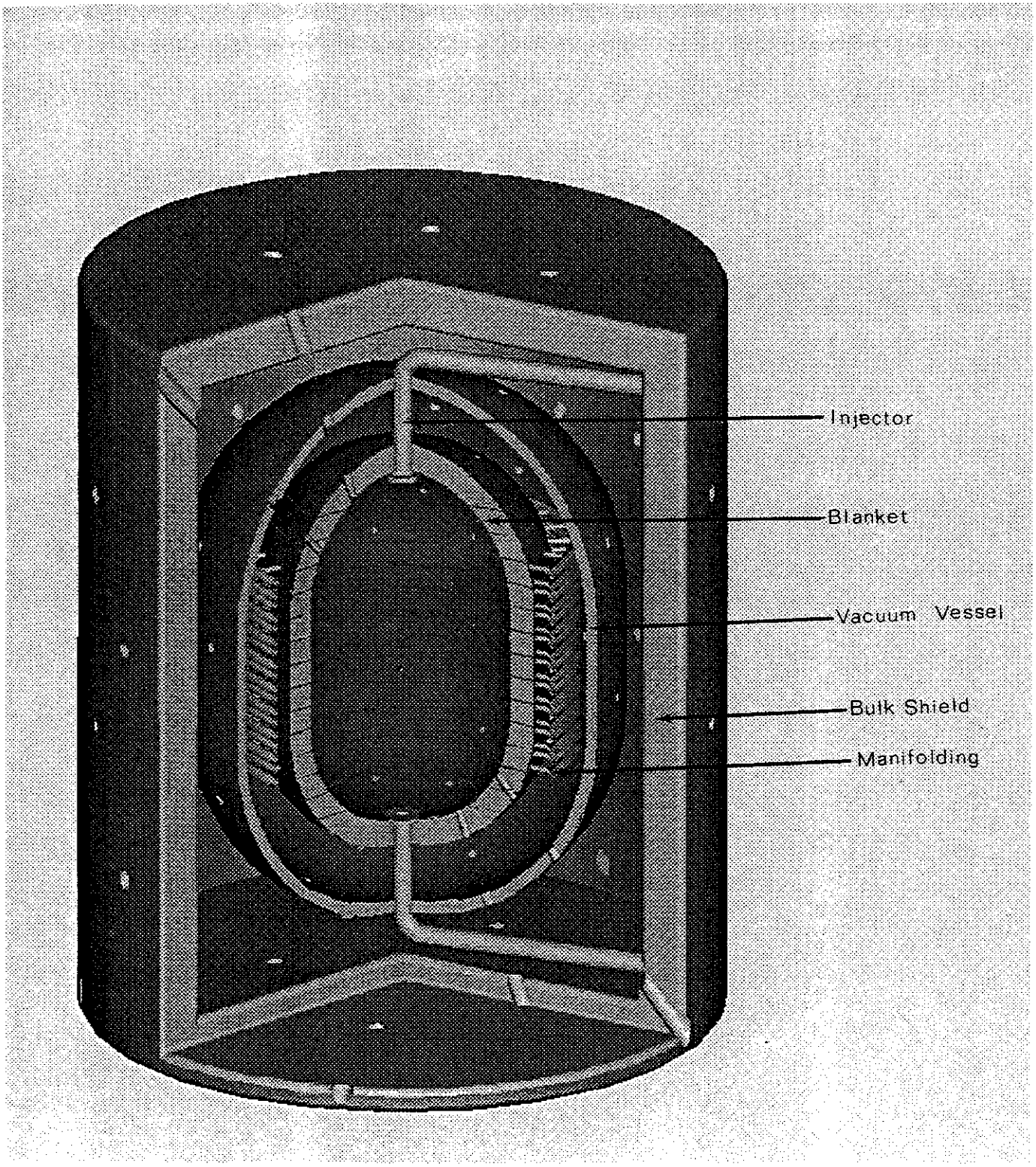

Figure 6.8-2. Perspective View of the Cavity without Laser Beams

McDonnell Douglas Aerospace

The SiC structure must be flexible enough to withstand cyclic loading from the blast, but strong enough to support itself and the internal pressure of the film. A supply region behind the porous structure serves to slowly feed the liquid and also to remove the heat from the first wall (40% of the total fusion power). Blast energy is removed from the cavity initially by evaporation. During the recondensation phase of each pulse, heat is conducted through the relatively thin film and into the first wall coolant.

Design of the Prometheus wetted wall concept considers several important first wall issues, including: (1) cavity vapor hydrodynamics; (2) limits on cavity clearing time due to the requirment to conduct heat out radially; (3) film flow uniformity, wetting, and drainage; and (4) mechanical response of the first wall system. A detailed description of the first wall system and analysis of the major issues are found in Section 6.8.2.

The first wall system and blanket are physically separated. The environmental conditions and functions performed by these two components are very different; separation allows for better optimization of performance, more flexibility, and good maintenance features. The blanket is protected from the blast and is designed to optimize breeding, energy conversion, reliability, and maintainability. The major penalty is the need for an attachment and locking mechanism and more complicated maintenance scheme.

The first wall system consists of individual plates which are locked into a support system attached to the blanket. The ability to provide removable panels which lock into the blanket is essential to allow more frequent maintenance of the first wall panels and still mitigate the mechanical effects of the blast by absorbing the loads into the blanket and support system.

The blanket consists of several rings through the cylindrical and hemispherical sections. Blanket modules are pre-assembled into the rings, which stack vertically on top of one another. At laser penetration holes, the corresponding module length is shortened to allow for penetration space. The blanket modules are made of SiC and contains a number of U-bend woven SiC tube sheets inside which the pressurized He coolant flows. The Li_2O is placed in packed bed form between the tube sheets and is purged by He flowing along the axis of the module. Use of Li_2O in conjunction with the first wall Pb coolant provide the potential for adequate tritium breeding without the need for Be as a multiplier. A more detailed description of the blanket is found in Section 6.8.3. Neutronics, thermal hydraulics, thermomechanics, and tritium analyses are presented.

The first wall and blanket are maintained by removing the upper end cap. The first wall panels can then be removed separately, or the entire blanket rings can be lifted. Preliminary analysis suggests that the first wall service life is of the order of five years, whereas the blanket might last ten years with the heavy ion option slightly less due to the higher power density.

Figure 6.8-3 shows the radial build from the first wall through the shield which is typical for both the -L and -H option. The cavity radius is nominally 4.5 m for the Prometheus-H cavity. Relatively large manifolding is needed behind the blanket to keep the He coolant pressure drop low. The manifolding is made from SiC composite up to the vacuum vessel and shield, where a transition is made to more conventional ferritic/martensitic steel. The vacuum vessel is also made of steel.

The radiation shield for Prometheus has been designed to protect components and personnel. It consists of (1) a bulk shield circumscribing the blanket, (2) penetration shielding around the driver beam lines and vacuum ducts, and (3) a biological shield, which also serves as the reactor building wall. The system was designed to achieve several goals: (a) the biological dose rate outside the reactor building during operation is below 2.5 mrem/hr, (b) neutron-induced activation in all components outside the blanket but inside the reactor building (e.g., heat transport system and steam generators) is minimized, and (c) the biological dose rate in the reactor building outside the blanket decays to <2.5 mrem/hr within 48 hours after shutdown in order to permit personnel access, if needed, although the reactor system is designed for fully-remote maintenance operations. More detail can be found in Section 6.8.4.

Safety and environmental issues are treated separately in Section 6.8.5. Safety and environmental concerns weighed heavily in the design choices made in Prometheus, and contribute to the overall attractiveness of the concept.

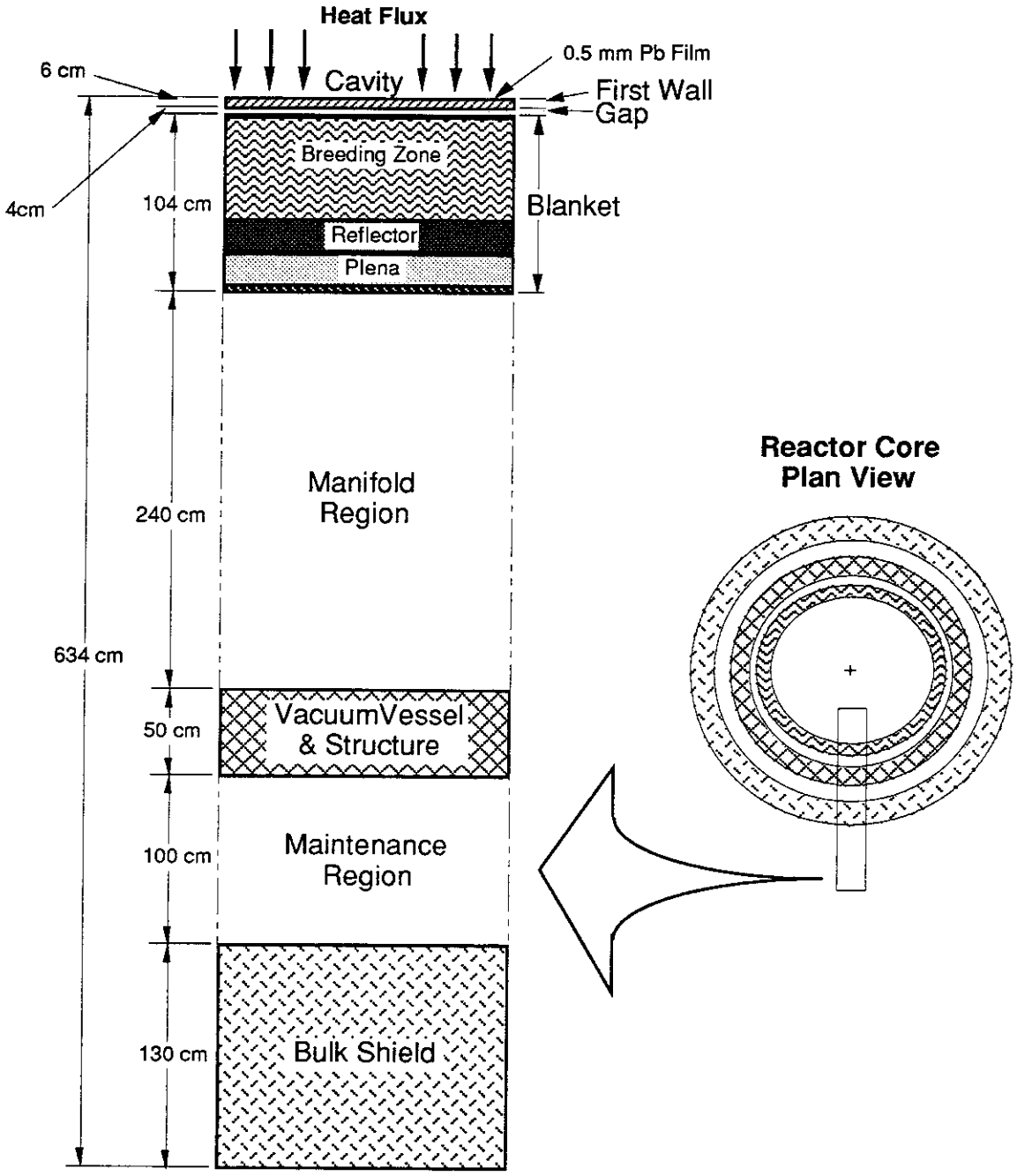

Figure 6.8-3 Radial Build of the Cavity

This page intentionally left blank.

6.8.1 Neutronics Analysis

6.8.1.1 Introduction – The energy and angular distributions of neutrons incident on the first wall of IFE reactors differ appreciably from those found in MFE reactors. Neutrons (and gamma-rays) generated from the microexplosion at the center of the cavity are incident perpendicular to the first wall, particularly if the chamber is close to spherical in shape, whereas in MFE reactors they impinge on the first wall with various incident angles. Thus, to produce the same wall load or fluence at the first wall (expressed either in MW/m^2 or $MW\text{-}y/m^2$), more neutrons are required in the case of MFE reactors as compared to ICF reactors. Furthermore, the incident neutrons in IFE reactors are degraded in energy (~12 MeV) due to their slowing down process in the target after the microexplosion, whereas in MFE their energies are rather well defined around 14.1 MeV. Therefore, more neutrons with degraded incident energies are required to produce a given wall load as compared to the MFE case. These angular and spectral differences impact the neutronics characteristics of the first wall and blanket systems, particularly the damage parameters in the first wall.

In the present study, target neutronics calculations were not performed. Instead, the incident neutron spectrum of the SIRIUS-M[1] reactor design was used. About 78% of the target neutrons are 14.1 MeV neutrons, 21% are in the energy range 3.5-14.1 MeV and ~1% are in the energy range 1.5 MeV-3.5 MeV. Thus, the average neutron energy incident on the first wall/blanket systems is ~12.87 MeV. No gamma-rays were considered from the target. In addition, time-dependent calculations were not performed. This neglects effects due to instantaneous heating or damage rates which are time-dependent due to differences in the arrival time of neutrons to the first wall.

Time-averaged values are reported below for the key parameters, including blanket power multiplication (M) and tritium breeding ratio (TBR).

6.8.1.2 Base Case Configuration – The cavity consists of four distinct systems: the first wall system, blanket/reflector/plena system, vacuum vessel, and bulk shield system. Figure 6.8.1-1 shows the compositions and radial build through the center of the cavity.

The first wall system carries away the energy deposited by the x-rays and debris, as well as the nuclear heating resulting from neutron and gamma-ray transport in the first wall system. Energy also is deposited in the lead film that covers the inner surface of the cavity. Lead is a good neutron multiplier and has been proposed for that purpose in several conceptual blanket designs.

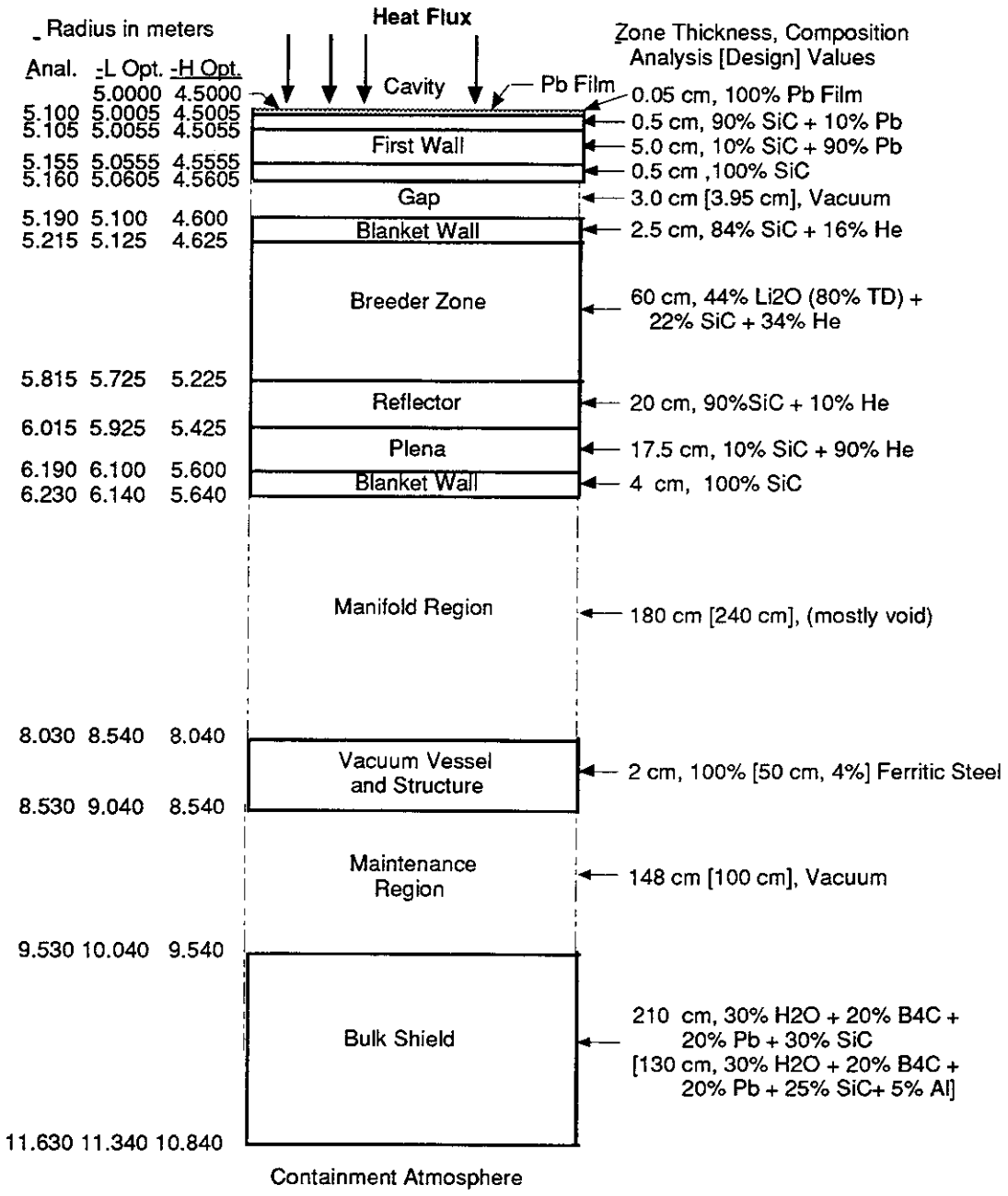

Figure 6.8.1-1 Material Composition in the 1-D Cavity Model

Beryllium was considered for use in the blanket to enhance the power multiplication and tritium production rate. Its neutron multiplication characteristics are superior to lead. Neutron multiplication basically occurs through (n,2n) reactions whose threshold energy is lower for beryllium (~2.8 MeV) than for lead (~7.5 MeV), although at ~12 MeV, the (n,2n) cross-section is larger in lead than in beryllium (~2 barns for lead, 0.5 barns for beryllium). With 5 cm of Pb in the first wall region, Be is not required in the blanket and so the baseline design has no Be.

Lead flows through near-rectangular channels in a zone of width 5 cm and has been optimized to have a large volume ratio of 9:1 compared with the structural material (SiC) in order to enhance tritium breeding ratio and power multiplication. A porous SiC first wall is used with ~10% by volume Pb seeping out to the inner surface of the cavity. The back wall of the first wall system is a 100% SiC of a thickness 0.5 cm.

The blanket/reflector/plena (BRP) system utilizes SiC everywhere as the structural material. Neutronically, SiC has lower absorption cross-section for neutrons as compared to iron-based structure, leading to a higher chance for neutrons to be absorbed in lithium. On the other hand, energy multiplication in steels is normally larger than in SiC due to the larger exothermic (n,γ) reactions in steels. However, the high activation level in steels is a concern which was one of the motivations behind selecting SiC as the structural material in Prometheus design. Additionally, SiC was selected as the reflector material behind the breeding zone due to the high neutrons reflectivity characteristics of carbon. The thickness of the breeding zone was selected to be 60 cm based on parametric analysis which is discussed in Section 6.8.3.3. It consists of 43.6% by volume Li_2O with theoretical density (T.D.) of 80%, 22% SiC, and helium as the coolant (34.4%). The blanket first wall is 2.5-cm thick and is cooled with helium (84%SiC, 16%He). The reflector and plena zones are 20-cm and 17.5-cm thick, respectively, with a 4-cm 100% SiC back wall.

The manifold region is assumed to be 180-cm thick and is mostly void. The vacuum vessel is 2-cm thick made of 100% ferritic steel, followed by a maintenance zone of 148 cm. The final design resulted in a manifold region 240-cm thick, a vacuum vessel 50-cm thick (4% steel), and a maintenance region 100-cm thick. The design of the bulk shield in Prometheus calls for allowing personnel access 48 hours after shutdown. The analysis used an effective shielding material made of 20%Pb, 20%B_4C, 30%SiC, and 30% water. The final design shield used 20% Pb, 20% B_4C, 25% SiC, 30% water, and 5% aluminum structure. The flux attenuation characteristics of this shielding material is approximately an order of magnitude reduction in neutron flux level every 20 cm (see Section 6.8.4). Based on adopting a flux level of 1×10^6 n/cm^2•sec at the back of the shield during operation such that personnel access is permitted 24 hours after shutdown (for a more conservative estimate, see

Section 6.8.4), the bulk shield thickness was estimated to be 130 cm. Reinforced concrete (87% concrete, 8% carbon-steel, and 5% water) was also examined as an option for the bulk shield material. The neutron flux attenuation characteristics for this material was calculated to be an order of magnitude reduction in the neutron flux level for every 25 cm. Thus, a thicker shield is required in this case as compared to the Pb/B_4C composite shield when personnel access to the inside of the reactor building is permitted one day after shutdown. By adopting this design criterion, the required bulk shield thickness in the concrete case is estimated to be 165 cm.

6.8.1.3 Results – The neutronics parameters of the base design were calculated by performing one-dimensional calculations in spherical geometry using the ANISN 1-D discrete ordinates transport code[2] along with the the MATXS5 (30-g neutrons, 21-g) library[3] based on ENDF/B-V nuclear data. The radial build is shown in Figures 6.8-1 and 6.8.1-1. Figure 6.8.1-1 also shows the material volume fractions used in the calculations. This final baseline design evolved from parametric studies presented in Section 6.8.3.3. Note that a bulk shield thickness of 210 cm was considered in the calculations, while a thinner shield was adopted in the final design as discussed above. It was shown that tritium breeding ratio and blanket power multiplication are insensitive to an increase in the bulk shield thickness beyond ~1 m.

The results reported here are based on an incident neutron power of 2027 MW in the laser reactor design (1,818 MW in the heavy ion design). For an average neutron energy of 12.87 MeV, the incident neutron source is estimated to be 9.83×10^{20} n/sec (8.82×10^{20} n/sec in the heavy reactor design). Also, while the first wall in the model shown in Figure 6.8.1-1 is placed at a radial distance of 510 cm from the cavity center, the cavity radius in the final laser reactor design is 500 cm. Thus, a correction factor of $(510/500)^2 \sim 1.04$ should be applied to the absolute local profiles reported here. Likewise, the cavity radius in the heavy ion reactor design is 450 cm, and the factor to be applied to local values in this case is $(510/450)^2 \cdot (8.82/9.83) \sim 1.15$.

Table 6.8.1-1 summarizes the key neutronics parameters for the baseline design of Prometheus-L and -H. The heating rates, power multiplication, damage rates in Si, and tritium production rates are described in more detail below.

Cavity Power Multiplication (M) and Nuclear Heating Rate Profiles – Figure 6.8.1-2 shows the nuclear heating rate in the baseline design as a function of the radial distance from the cavity center. Figures 6.8.1-3, 6.8.1-4, and 6.8.1-5 show these heating profiles in the first wall system, the blanket/reflector/plena system, and the bulk shield system (concrete case), respectively.

Table 6.8.1-1 Key Neutronics Parameters for Prometheus-L and Prometheus-H

	-L	-H
^{6}Li Enrichment	25%	25%
TBR	1.2	1.2
Li Annual Burnup	0.5%	0.6%
Peak-to-Average Burnup	3	3
Net Power Multiplication	1.14	1.14
Peak Power Densities (MW/m^3)		
Pb Film	32	37
Pb Coolant	28	32
First Wall	24	28
Breeder	20	23

In the first wall system, the largest power density takes place in the lead film covering the inner surface of the cavity since this film is the first material zone to intercept the highly energetic neutrons resulting from the blast. The power density in this film is ~32 MW/m^3 and is due mainly to heat deposited by gamma rays produced by neutron interactions with lead, particularly inelastic scattering reactions. The energy deposited by these gamma rays is ~25 MW/m^3 while the energy deposited by neutrons is only ~8 MW/m^3. Gamma-ray heating also dominates the total heating rate in the lead channel zone (by ~80%) where the average total heating rate is ~25 MW/m^3. The total heating rate in the first wall (90%SiC, 10%Pb) is 24 MW/m^3 and is dominated by neutron heating (~75%) as can be seen from Figure 6.8.1-3.

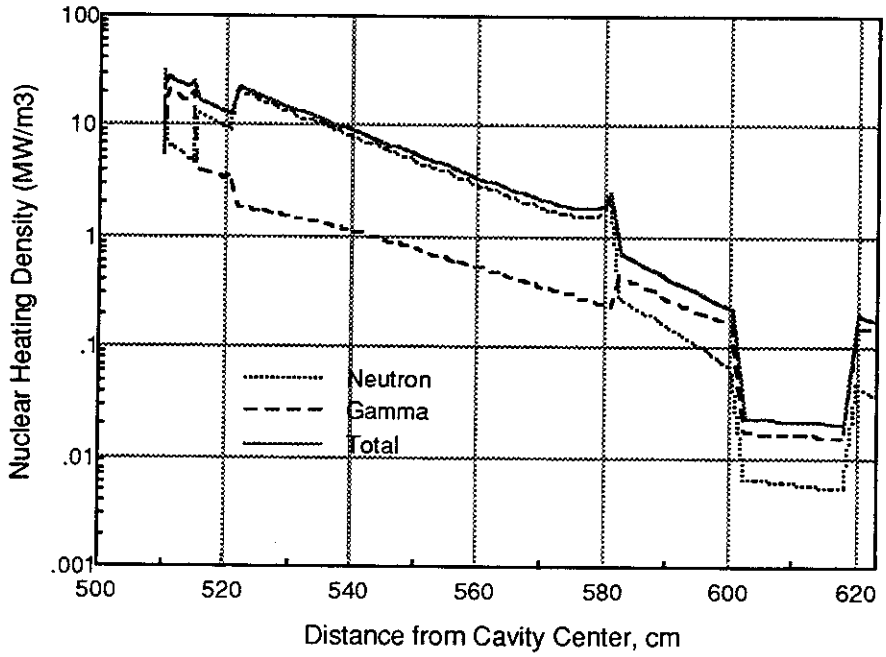

Figure 6.8.1-2. Nuclear Heating Rate Profile in the Baseline Design

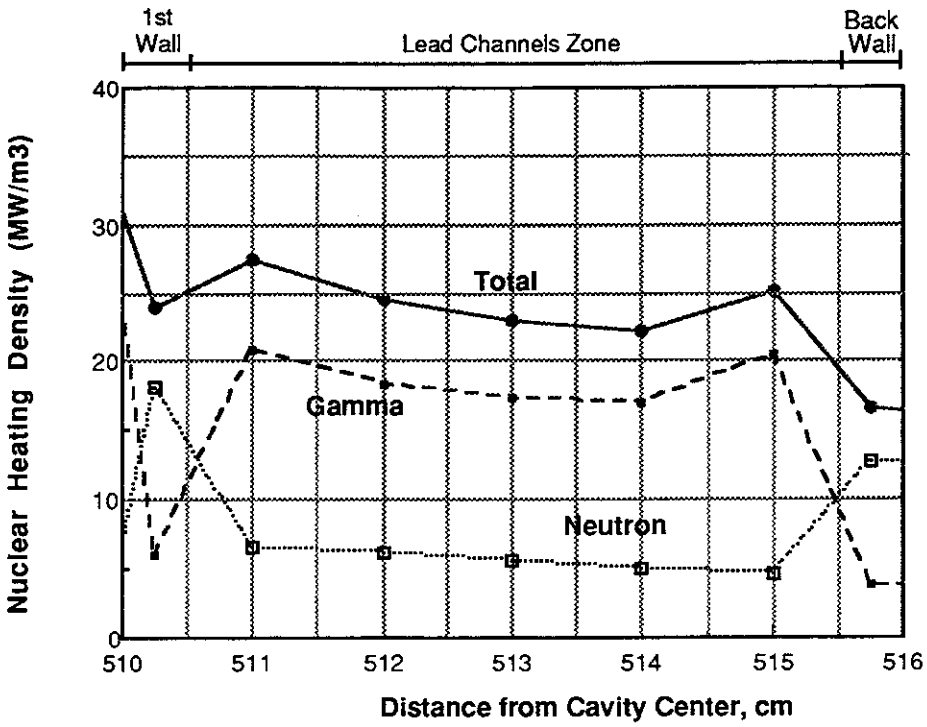

Figure 6.8.1-3 Nuclear Heating Rate Profile in the First Wall System

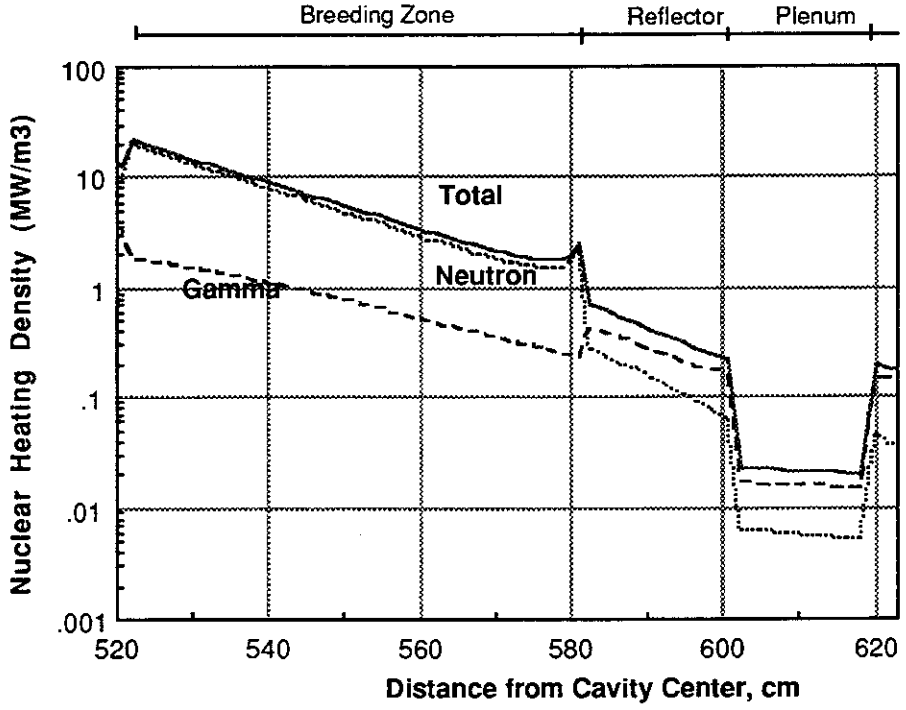

Figure 6.8.1-4 Nuclear Heating Rate Profile in the Blanket/Reflector/Plena System

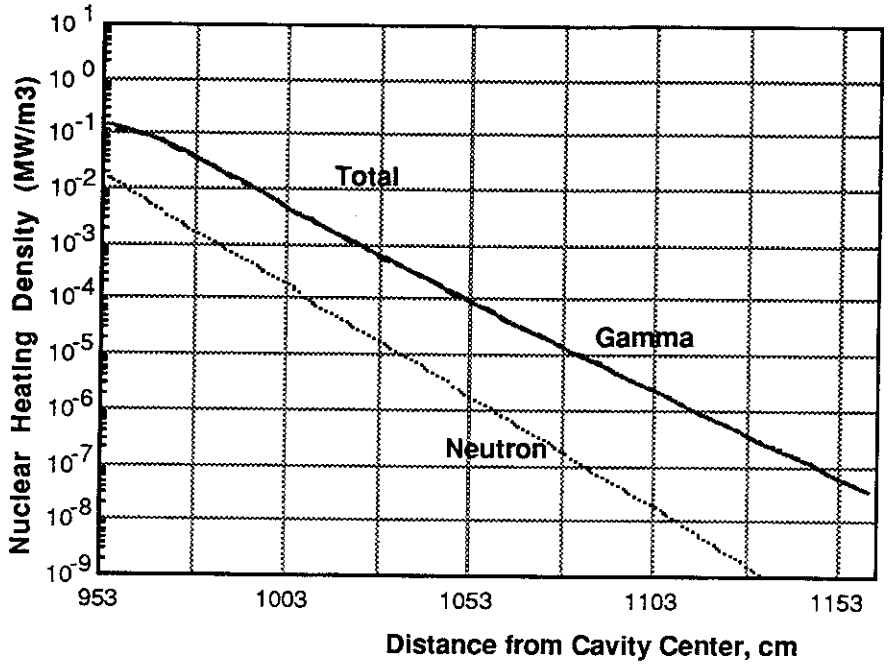

Figure 6.8.1-5 Nuclear Heating Rate Profile in the Concrete Bulk Shield Case

The largest nuclear heating rate in the breeding zone is ~20 MW/m^3 just behind the first wall of the blanket/reflector/plena system (see Figure 6.8.1-4). In the breeding zone, nuclear heating is mainly due to neutron absorption events in ^{6}Li through the tritium producing reactions, (n,α), for an enrichment of 25% in ^{6}Li. This enrichment level was shown to be the optimal value for larger TBR (see Section 6.8.3.3). The power density in the first wall of the blanket (cooled with helium) is ~12 MW/m^3. The average heating rates in the reflector and the plena regions are ~0.5 MW/m^3 and ~0.02 MW/m^3, respectively. The attainable heating rate level in the vacuum vessel is ~0.5 MW/m^3.

Total heating rate in the bulk shield is generally low. In the concrete shield case, the maximum heating rate at the front edge of the shield is ~0.15 MW/m^3 and the local values drop noticeably by distance (see Figure 6.8.1-5). After 1 m depth, the local heating rate drops ~3 orders of magnitude; that is, an order of magnitude reduction in local heating takes place for every ~33 cm. The nuclear heating in this type of shielding material is mainly due to gamma-ray heating. The gamma flux level in this concrete shield is about 1-2.5 orders of magnitude larger than the neutron flux level, with a larger difference (a factor of 2.5) occurring at a depth of ~165 cm (see Section 6.8.4).

As is shown in Section 6.8.4, the gamma flux in the concrete shield attenuates slower than the neutron flux during operation. The nuclear heating profile in the concrete shield (dominated by gamma-ray heating) has the same attenuation characteristics as the gamma flux and biological dose (in mremlhr) which is an order of magnitude reduction in their values occurs for about every 33 cm. At a distance of 165 cm, the heating rate is as low as ~10^{-6} MW/m^3.

Table 6.8.1-2 summarizes the fraction of power deposited in the various zones of the cavity. In the table, the integrated power is expressed in Joules per incident source neutron and, thus, the entries are independent of the total fusion power, neutron yield, etc. To convert the entries given in Table 6.8.1-2 to absolute values (in MW), the following formula could be used:

(power deposited, J/n) • (incident neutron power, MW) • 4.85 x 10^{11}

or alternatively,

(% of power deposited, by zone) • (incident neutron power, MW) • 1.14,

where the cavity power multiplication factor, M, is ~1.14. The total nuclear power in the cavity is the product of the incident neutron power and the cavity power multiplication, M.

In the case of the laser reactor (neutron power ~2027 MW), the cavity nuclear power is 2311 MW. It is ~2073 MW in the heavy ion reactor design. As shown in Table 6.8.1-2, ~21% of this power is deposited in the first wall system while ~77% is deposited in the blanket/reflector/plena system. The fraction of the cavity nuclear power deposited in the bulk shield is low (1.4%).

Table 6.8.1-3 summarizes the cavity energy balance, assuming a yield of 497 MJ and repetition rate of 5.6 Hz for the laser reactor while these values are 719 MW and 3.5 Hz in the heavy ion reactor, respectively. The fraction of the fusion power (2807 MW) in the laser reactor carried away by neutrons, debris, and x-rays are 72.23%, 21.53%, and 6.24%, respectively. These fractions are slightly different in the heavy ion reactor whose fusion power is ~2543 MW. The power load in the first wall system includes both surface heating (from the x-rays and debris) and the nuclear heating resulting from neutrons and gamma-ray interactions with the first wall system materials. By accounting to the power loads in the various components of the cavity, the total thermal power is 3092 MW in the laser reactor case and 2797 MW in the heavy ion reactor case.

Table 6.8.1-2 Nuclear Heating in Prometheus First Wall/Blanket/Shield Systems (Per Incident Neutron)*

System	Zone Number	Zone Name	Material Composition	Thickness (cm)	Power Deposited J/neutron	% (by zone)	% (by system)
First Wall Protection System		Lead film	100% Pb	0.05	5.345-15	0.288	
	1	Front SiC Layer	90% SiC, 10% Pb	0.5	4.084-14	1.743	
	2	Lead tubes	10% SiC, 90% Pb	5	4.188-13	17.869	
	3	Back SiC Layer	100% SiC	0.5	2.896-14	1.236	(21.076)
Gap	4	Vacuum	—	3	—	—	(0)
Blanket/Reflector System	5	Blanket First Wall	84% SiC, 16% He	2.5	1.142-13	4.873	
	6	Breeding Zone	43.6% Li2O, (0.8 TD), 22% SiC, 34.4% He	60	1.649-12	70.359	
	7	Reflector	90% SiC, 10% He	20	3.795-14	1.619	
	8	Plenum	10% SiC, 90% He	17.5	1.834-15	0.078	
	9	Back SiC Wall	100% SiC	4	3.758-15	0.160	(77.089)
Manifolds	10	Vacuum	—	180	—	—	(0)
Vacuum Vessel and Structure	11	Vacuum Vessel	100% Ferritic Steel in the first 2 cm, rest is vacuum	50	9.101-15	0.388	(0.388)
Maintenance Gap	12	Vacuum	—	100	—	—	(0)
Bulk Shield	13	Reinforced concrete cooled with water	87% Concrete 8% Ferritic Steel 5% Water	210	3.386-14	1.445	(1.445)
Total					2.347-12	100	100
Power Multiplication (M)					(1.14)+		

* Entries given are per incident source neutron.

\+ Evaluted as energy deposited in the entire system (MeV) divided by the average energy per incident source neutron (of SIRIUS-M type) of ~12.87 MeV

(1) Read as 5.345×10^{-15}

Damage Rate Profile – Figure 6.8.1-6 shows the displacement per atom (dpa) per full power year (FPY) in silicon as a function of distance from the cavity center. In the 0.5-cm thick first wall (90% SiC, 10%Pb), the maximum dpa rate in silicon is ~127 dpa per full power year based on 9.83×10^{20} n/sec incident neutron source of an average energy of 12.87 MeV in the laser reactor. This value is ~146 dpa/FPY in the heavy ion reactor. The average wall loads in the laser reactor is 6.5 MW/m^2 and 7.3 MW/m^2 in the heavy ion reactor. The dpa rate in the first wall of the blanket (2.5-cm thick, 84%SiC, 16%He) is ~85 dpa/FPY in the laser reactor and is ~98 dpa/FPY in the heavy ion reactor design.

Table 6.8.1-3 Cavity Energy Balance

	Laser	Heavy Ion	Units
Total Yield	497	719	MJ
Repetition Rate	5.65	3.54	Hz
Fusion Power	2807	2543	MW
Yield Distribution			
X-ray	6.24	6.40	%
Debris	21.53	22.11	%
Neutrons	72.23	71.49	%
Yields			
X-rays	31	46	MJ
Debris	107	159	MJ
Neutrons	359	514	MJ
Power			
Surface Heating	780	725	MW
Neutrons	2027	1818	MW
Neutron Source Strength*	9.83×10^{20}	8.82×10^{20}	n/sec
FW/Blanket/Shield Characteristics			
TBR	1.2	1.2	
Power Multiplication	1.14	1.14	
Nuclear Power	2311	2073	MW
Nuclear Power Distribution			
First Wall System	21.1	21.1	%
Blanket/Reflector/Plenum	77.1	77.1	%
Vacuum Vessel	0.4	0.4	%
Shield	1.4	1.4	%
Power Loads			
First Wall System	1268	1162	MW
Blanket/Reflector/Plenum	1782	1598	MW
Vacuum Vessel	9.2	8.3	MW
Shield	32.4	29	MW
Total Thermal Power	3092	2797	MW

* Average incident neutron energy ~12.87 MeV

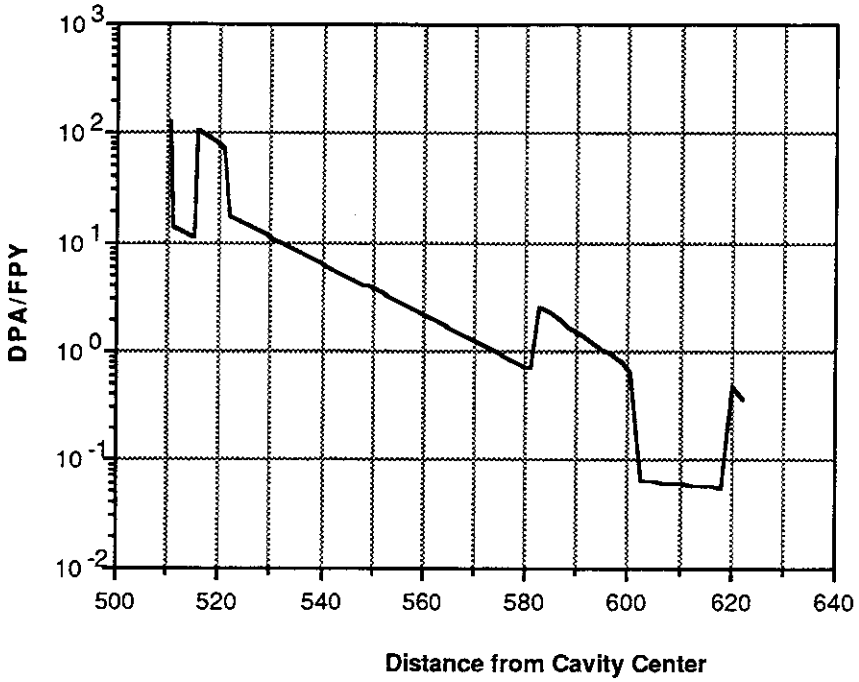

Figure 6.8.1-6 Displacement Per Atom Per Full Power Year (dpa/FPY) in Silicon

Tritium Breeding Ratio (TBR) and Tritium Production Profiles – Based on the parametric studies reported in Section 6.8.3.3 on the variation of the TBR as a function of the ^{6}Li enrichment, lead zone thickness in the first wall system, and the breeding zone thickness, the optimal value attainable in the base design is TBR ~1.2. The profiles for tritium production rate (TPR) from ^{6}Li (T-6) and from ^{7}Li (T-7) are shown in Figure 6.8.1-7. The TPR from ^{6}Li is more than an order of magnitude larger than the TPR from ^{7}Li just behind the first wall of the blanket/reflector/plena system and this difference narrows towards the back locations in the breeding zone. The T-7 profile is more or less steady throughout the blanket while T-6 profile is steep, particularly at the front locations in the breeding zone.

Neutron Spectrum - The neutron flux in the first wall of the FWS and in the first wall of the blanket/reflector/plena system is shown in Figure 6.8.1-8 for each of the energy groups (30-group) used in the 1-D transport calculations for the baseline configuration. The results shown are expressed in terms of flux per incident source neutron ($n/cm^2 \cdot sec \cdot n$). Figure 6.8.1-9 shows the absolute values of the flux ($n/cm^2 \cdot sec$) for incident neutron source of 9.83×10^{20} n/sec which corresponds to neutron power of 2027 MW in the laser reactor design. In the heavy ion reactor, the absolute values of the flux can be obtained from Figure 6.8.1-9 (and Figure 6.8.1-11 below) by applying a factor of 1.15. The total neutron flux is the summation of each group flux shown in Figures 6.8.1-8 and 6.8.1-9.

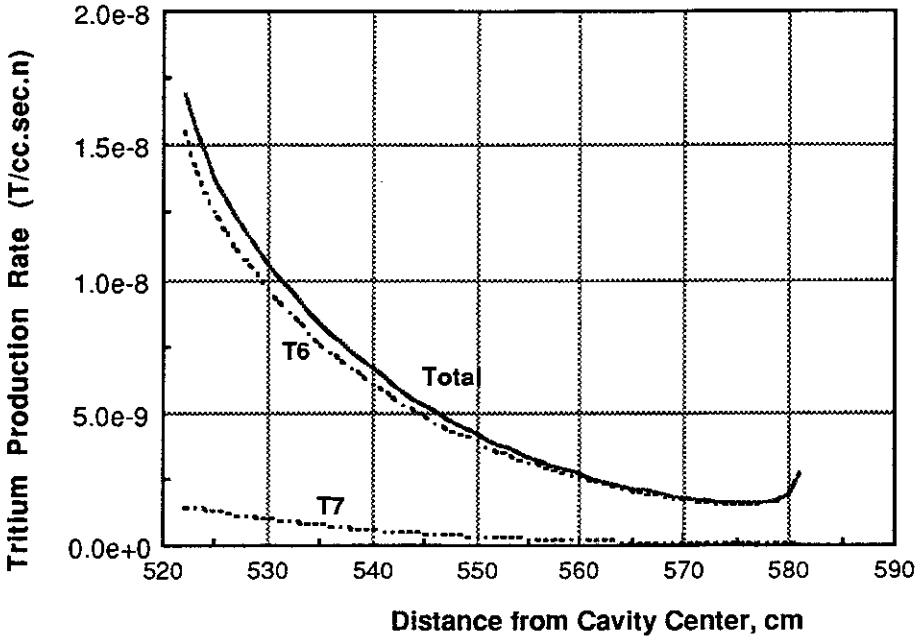

Figure 6.8.1-7 Tritium Production Rate (TPR) Profile in the Breeding Zone Per Incident Neutron

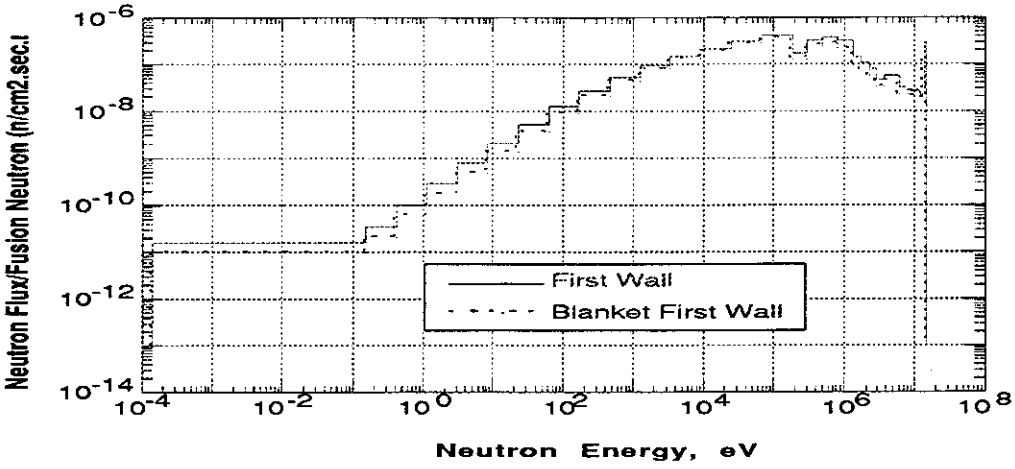

Figure 6.8.1-8. Neutron Flux (by Group) in the First Wall of the FWS and in the First Wall of the Blanket/Reflector/Plena System per Incident Neutron

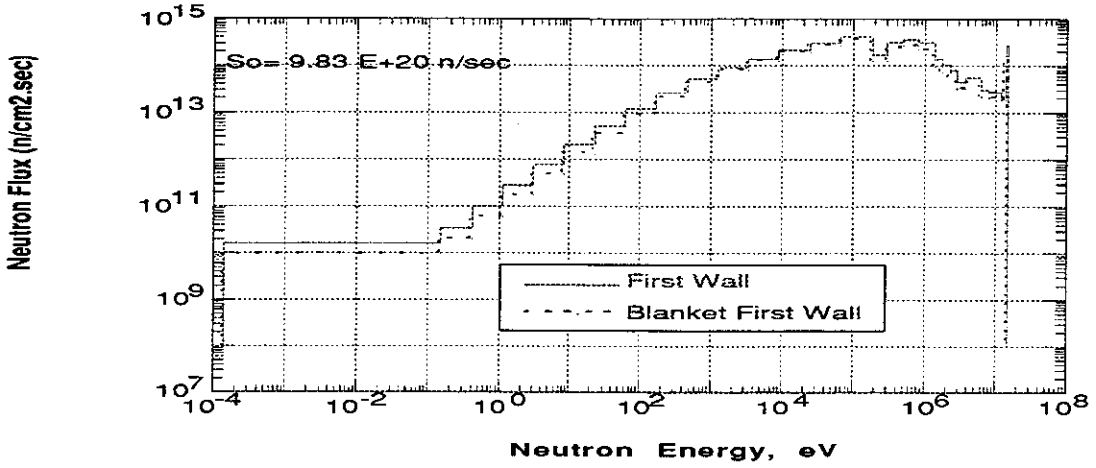

Figure 6.8.1-9. Neutron Flux (by Group) in the FW of the FWS and the FW of the Blanket/Reflector/Plena System (n/cm2•sec)

The fraction of the uncollided neutrons (14.1 MeV) that are confined in the first energy group (13.5 MeV-15.0 MeV) of the total flux (3.22×10^{15} n/cm^2•sec) in the FW of the FWS is ~8.6%. This is to be compared to the percentage of the 14.1 MeV neutrons in the incident neutron source which is ~78%. This indicates that an appreciable softer neutron component exists in the total flux in the FW due to neutrons colliding with the FWS materials (and blanket) and reflected back to the first wall. The total neutron flux above 0.2 MeV in the FW of the FWS is ~1.97×10^{15} n/ cm^2•sec and is ~1.37×10^{15} n/cm^2•sec in the FW of the B/R/P system. These neutrons represent ~61% and ~55% of the total neutron flux at these locations, respectively. (The total neutron flux in the FW of the B/R/P system is ~2.47×10^{15} n/cm^2•sec.) Most of these neutrons are in the energy range 0.2 MeV-2.2 MeV (~46% and ~43% of the total flux, respectively).

Figure 6.8.1-10 and 6.8.1-11 show the neutron flux above 0.2 MeV per source neutron and for incident neutron source of 9.83×10^{20}n/sec. The total fluxes above 0.2 MeV are 1.97×10^{15} n/cm^2•sec and 1.37×10^{15} n/cm^2•sec in the FW and in the FW of the B/R/P systems, respectively. The corresponding fluxes in the heavy ion reactor are 2.27×10^{15} n/cm^2•sec and 1.58×10^{15} n/cm^2•sec. These fluxes were used to estimate the lifetime of the FWS and the blanket.

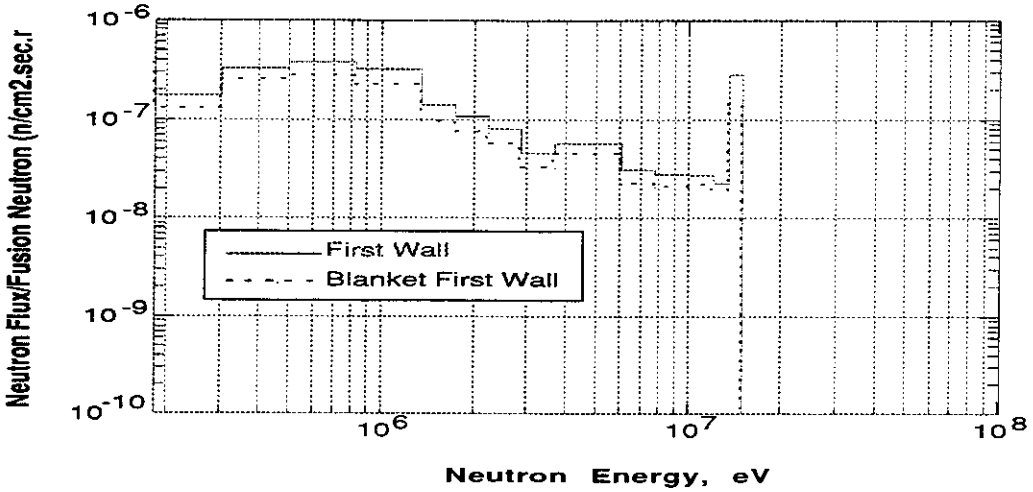

Figure 6.8.1-10: Neutron Flux Above 0.2 MeV in the FW of the FWS and in the FW of the Blanket/Reflector/Plena System per Incident Neutron (n/cm2•sec•n)

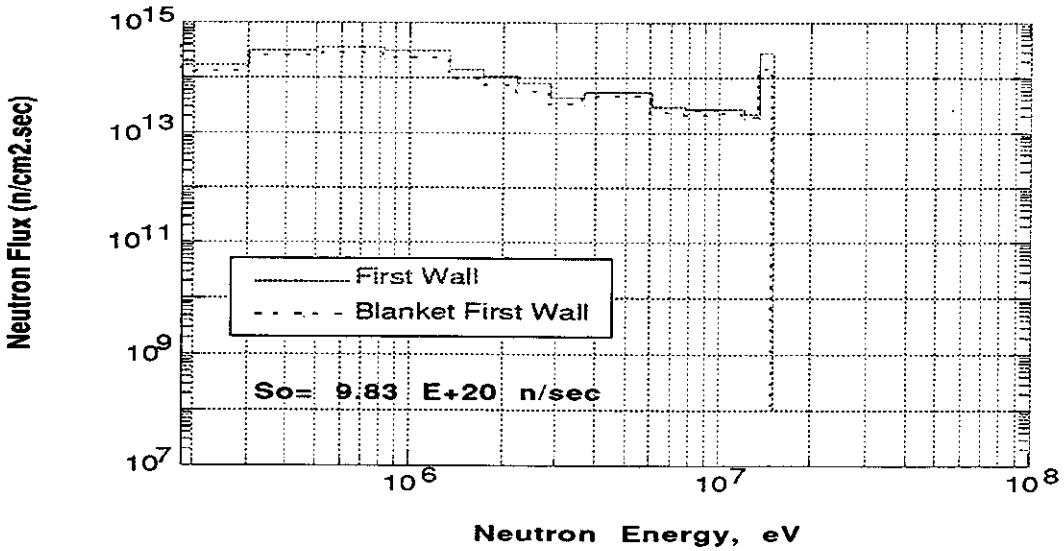

Figure 6.8.1-11: Neutron Flux (by Group) in the FW of the FWS and in the FW of the Blanket/Reflector/Plena System (n/cm2•sec)

References for 6.8.1

1. B. Badger, et al.,"SIRIUS-M: A Symmetric Illumination, Internally Confined Direct Drive Material Test Facility," UWFDM-711, Fusion Technology Institute, University of Wisconsin, October 1986.

2. W. W. Engle, Jr., "A User's Manual for ANISN," K-1693 (1967).

3. R. E. MacFarlane, " TRANSX-CTR: A Code for Interfacing MATXS Cross-Section Libraries to Nuclear Transport Codes for Fusion Systems Analysis," LA-9863-MS, Los Alamos National Laboratory, February 1984.